

Conditional Panoramic Image Generation via Masked Autoregressive Modeling

Chaoyang Wang¹, Xiangtai Li¹, Lu Qi², Xiaofan Lin²,
Jinbin Bai³, Qianyu Zhou⁴, Yunhai Tong¹

¹Peking University, ²Insta360 Research, ³National University of Singapore, ⁴Jilin University

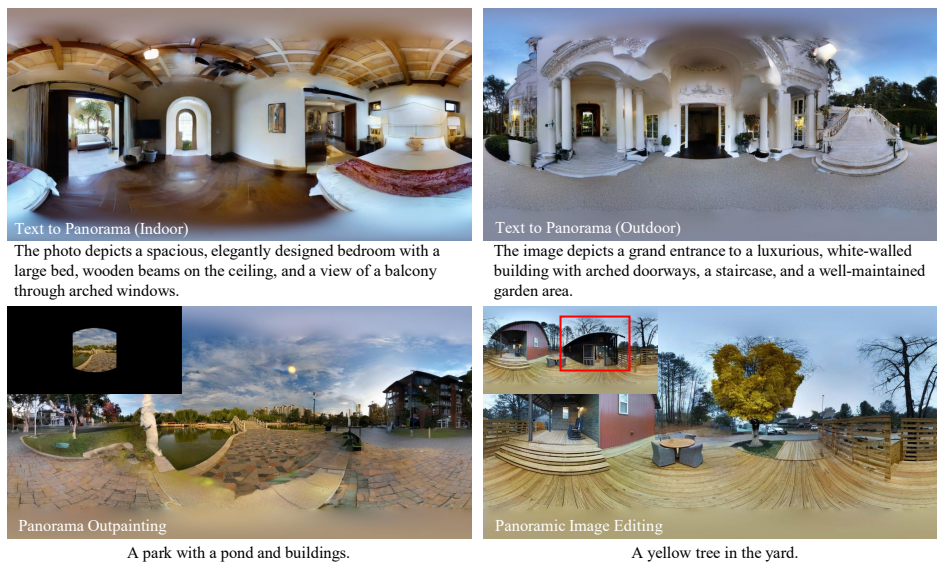


Figure 1: **Generated samples from Panoramic AutoRegressive (PAR) Model.** PAR unifies several conditional panoramic image generation tasks, including text-to-panorama, panorama outpainting, and panoramic image editing.

Abstract

Recent progress in panoramic image generation has underscored two critical limitations in existing approaches. First, most methods are built upon diffusion models, which are inherently ill-suited for equirectangular projection (ERP) panoramas due to the violation of the identically and independently distributed (*i.i.d.*) Gaussian noise assumption caused by their spherical mapping. Second, these methods often treat text-conditioned generation (text-to-panorama) and image-conditioned generation (panorama outpainting) as separate tasks, relying on distinct architectures and task-specific data. In this work, we propose a unified framework, Panoramic AutoRegressive model (PAR), which leverages masked autoregressive modeling to address these challenges. PAR avoids the *i.i.d.* assumption constraint and integrates text and image conditioning into a cohesive architecture, enabling seamless generation across tasks. To address the inherent discontinuity in existing generative models, we introduce circular padding to enhance spatial coherence and propose a consistency alignment strategy to improve generation quality. Extensive experiments demonstrate competitive performance in text-to-image generation and panorama

outpainting tasks while showcasing promising scalability and generalization capabilities. Project Page: <https://wang-chaoyang.github.io/project/par>.

1 Introduction

Panoramic image generation [1, 11, 12, 17, 18] has recently emerged as a pivotal research direction in computer vision, driven by its capability to capture immersive 360-degree horizontal and 180-degree vertical fields of view (FoV). This unique visual representation closely mimics human panoramic perception, enabling transformative applications across VR/AR [33, 76], autonomous driving [42], visual navigation [5, 24], and robotics [43, 58].

Despite some progress in recent years, existing panorama generation methods [17, 54, 55, 71, 67, 26, 35, 59, 75, 62, 61, 74] predominantly rely on diffusion-based base models and face two significant problems: task separation and inherent limitations of the modeling approach. First, different panoramic generation tasks are highly bound to specific foundation models. For instance, most text-to-panorama models [17, 54, 55, 71, 67] are based on Stable Diffusion (SD) [46, 41] while panorama outpainting models [26, 35, 59] are fine-tuned on SD-inpainting variants, resulting in task-specific pipelines that lack flexibility. Second, diffusion-based models struggle to handle the unique characteristics of equirectangular projection (ERP) panoramas, which map spherical data onto a 2D plane, violating the *i.i.d.* Gaussian noise assumption.

In addition to these fundamental issues, redundant modeling in existing methods introduces unnecessary computational costs. This redundancy manifests in several ways: 1) Some approaches [28, 35] iteratively inpaint and warp local areas, leading to error accumulation over successive steps. 2) Others [71, 53] adopt a dual-branch structure, with global and local branches, where the local branches are not directly used as final output targets. These challenges highlight the lack of a simple, unified, and efficient paradigm for conditional panoramic image generation.

In this work, we explore a powerful yet much less explored panoramic image generation paradigm to address the above limitations - the violation of *i.i.d.* assumption and the lack of unification. Moreover, we allow the model to take text or images as input and control the generated content at any position on the canvas. As shown in Fig. 1, PAR is competent for text-to-panorama, panorama outpainting, and editing tasks. Notably, our PAR requires no task-specific data engineering - both conditions are seamlessly integrated via a single likelihood objective. In comparison, Omni² [65] relies on meticulously designed joint training datasets to align heterogeneous tasks, inevitably introducing complexity and domain bias.

For this goal, inspired by masked autoregressive modeling (MAR) [29], we propose PAR. On the one hand, it is based on AR modeling, which avoids the constraints of *i.i.d.* assumptions. On the other hand, it allows for generation in arbitrary order, overcoming the shortcoming of traditional raster-scan methods that are incapable of image-condition generation. This flexibility of PAR unifies conditional generation tasks - panorama outpainting reduces to a subset of text-to-panorama synthesis, where existing image tokens serve as partially observed sequences. Building upon the MAR-based generative framework, we introduce two critical enhancements to address inherent limitations in standard architectures. First, conventional VAE-based compression often exhibits spatial bias during encoding-decoding: center regions benefit from contextual information across all directions, while peripheral pixels suffer from unidirectional receptive fields, contradicting the cyclic nature of ERP panoramas. To mitigate this, we propose *dual-space circular padding*, applying cyclic padding operations in both latent and pixel spaces. This ensures seamless feature propagation across ERP boundaries, aligning geometric and semantic continuity. Second, as the foundation model is pre-trained on massive perspective images, we devise a *translation consistency loss*. This loss explicitly regularizes the model to accommodate the prior of ERP panoramas by minimizing discrepancies between the model’s outputs under shifted and original inputs. Ultimately, two innovations holistically reconcile the unique demands of 360-degree imagery with the flexibility of MAR modeling. Experiments demonstrate that PAR outperforms specialist models in the text-to-panorama task, with 37.37 FID on the Matterport3D dataset. Moreover, on the outpainting task, it has better generation quality and avoids the problem of repeated structure generation. Ablation studies demonstrate the model’s scalability in terms of computational cost and parameters, as well as its generalization to out-of-distribution (OOD) data and other tasks, such as zero-shot image editing.

Our contribution can be summarized as follows: 1) We propose PAR, which fundamentally avoids the conflict between ERP and *i.i.d.* assumption raised by diffusion models, and also seamlessly integrates text and image-conditioned generation within a single architecture. 2) To enforce better adaptation to the panorama characteristic, we propose specialized designs, including dual-space circular padding and a translation consistency loss. 3) We evaluate our model on popular benchmarks, demonstrating competitive performance in text and image-conditional panoramic image generation tasks and showcasing its scalability and generalization capabilities.

2 Related Work

Conditional Panoramic Image Generation. There are two primary task paradigms in this area: 1) text-to-panorama (T2P), which synthesizes 360-degree scenes from textual descriptions, and 2) panorama outpainting (PO), which extends partial visual inputs to full panoramas. Given the success of diffusion models (DMs) [30, 31, 32, 41, 46, 49, 50] on generation tasks, such as image generation [46, 72, 22, 41, 40, 16], image editing [3, 36, 47, 73], image super resolution [21, 48, 68], video generation [2, 19, 66], current approaches typically build upon DMs, yet face two problems. First, DM is inherently unsuitable for panorama tasks due to reliance on the *i.i.d.* Gaussian noise assumption, which ERP transformations violate. Second, existing approaches lack task unification. Specifically, T2P methods typically fine-tune SD, while PO solutions adapt the SD-inpainting variants. Although some work [65] attempts a unified solution, it is based on DM and relies on complex task-specific data engineering. From a methodological perspective, existing methods can be divided into bottom-up and top-down. The former generates images with limited FoV sequentially [28, 35] or simultaneously [55, 26] and finally stitches them together, but faces the problem of lacking global information and error accumulation. The latter [71, 53] usually adopts a dual-branch architecture including a panorama and a perspective branch. However, this design brings unnecessary computational cost. In parallel, there are several AR-based attempts. They either rely on large DMs for final generation [35, 18], are limited to low resolution with additional up-sampling modules [9], or stitch perspective images without correct panorama geometry [77]. Overall, existing methods do not provide a unified and theoretically sound solution for conditional panorama generation, which we rethink through MAR modeling.

Autoregressive Modeling. Motivated by the success of large language models (LLMs) [4, 56], AR models, with great scalability and generalizability, are becoming a strong challenger to diffusion models. Several studies delve into visual AR with two distinct pipelines. One pipeline adopts raster-scan modeling [51, 45, 14, 15, 69, 60, 64, 27, 38], which treats the image as visual sentences and sequentially predicts the next token. However, this strategy does not fully exploit the spatial relationships of images. To make up for the shortcomings of raster-scan modeling, some works [6, 23, 70, 57, 29, 13] extend the concept of masked generative models [7] to AR modeling, namely MAR. Instead of predicting one token within one forward, the model randomly selects several candidate positions and predicts attending to the decoded positions. Intuitively, this modeling provides flexible control over arbitrary spatial positions simply by adjusting the order of tokens to be decoded. Hence, we resort to MAR as a flexible way to unify text and image-conditioned panorama generation while avoiding the theoretical defects of panorama DMs.

3 Method

This section is organized into three parts. First, we introduce the preliminaries of panorama projection and review the standard conditional AR modeling. Second, we analyze the disadvantages of this approach for unified conditional generation. Last, we describe our PAR in the following sections, including vanilla MAR architecture, consistency alignment, and circular padding.

3.1 Preliminaries

Equirectangular Projection is a common parameterization for panoramic images. It establishes a bijection between spherical coordinates (θ, ϕ) and 2D image coordinates (u, v) , where $\theta \in [0, \pi]$ denotes the polar angle (latitude) and $\phi \in (-\pi, \pi]$ represents the azimuthal angle (longitude). This projection preserves complete spherical visual information while maintaining compatibility with conventional 2D convolutional operations. Given a 3D point $\mathbf{P} = (x, y, z)$ on the unit sphere \mathbb{S}^2 , we

first compute its spherical coordinates and then obtain ERP coordinates (u, v) via linear mapping:

$$\phi = \arctan\left(\frac{y}{x}\right), \quad \theta = \arccos(z), \quad u = \frac{\phi + \pi}{2\pi}W, \quad v = \frac{\theta}{\pi}H, \quad (1)$$

where $W \times H$ denotes the target image resolution.

Conditional Autoregressive Models formulate conditional data generation as a sequential process through next token prediction. Given an ordered sequence of tokens $\{x_t\}_{t=1}^T$, the joint distribution $p(x|c)$ factorizes into a product of conditional probabilities:

$$p(x|c) = \prod_{t=1}^T p(x_t|x_{<t}, c), \quad (2)$$

where $x_{<t} \equiv (x_1, \dots, x_{t-1})$ denotes the historical context and c indicates the conditions. This chain rule decomposition enables tractable maximum likelihood estimation, with the model parameters θ optimized to maximize:

$$\mathcal{L}(\theta) = \mathbb{E}_{x \sim \mathcal{D}} \left[\sum_{t=1}^T \log p_{\theta}(x_t|x_{<t}, c) \right], \quad (3)$$

where \mathcal{D} represents the data distribution.

3.2 Rethinking Conditional Panoramic Image Generation

While DMs have demonstrated remarkable success in various image generation tasks, they rely on *i.i.d.* Gaussian noise assumption, which is violated by the spatial distortions introduced by the ERP transformation in Eq. 1, making diffusion-based methods inherently unsuitable for modeling panoramas. In this work, we therefore rethink conditional panorama generation from AR modeling, which is not constrained by such assumptions.

Building upon the standard conditional AR formulation in Eq. 2, we analyze text-to-panorama and panorama outpainting scenarios. The former takes text embeddings as c while the latter takes observed image patches and optional textual prompts as conditions. In particular, this reformulates the two problems as follows:

$$p(x|c) = \prod_{t \in \mathcal{S}_u} p(x_t|x_{\mathcal{S}(t)}, c), \quad \mathcal{S}(t) \subseteq (\mathcal{S}_k \cup \{1, \dots, t-1\}), \quad (4)$$

where \mathcal{S}_k denotes known token positions from the condition and $\mathcal{S}_u = \{1, \dots, T\} \setminus \mathcal{S}_k$ are targets. The context set $\mathcal{S}(t)$ dynamically aggregates:

$$\mathcal{S}(t) = \underbrace{\{j|j \in \mathcal{S}_k\}}_{\text{condition}} \cup \underbrace{\{j|j < t, j \in \mathcal{S}_u\}}_{\text{generated content}}, \quad (5)$$

This formulation generalizes text-to-panorama ($\mathcal{S}_k = \emptyset$) and outpainting ($\mathcal{S}_k \neq \emptyset$) scenarios. However, traditional raster-scan modeling is not competent for the panorama outpainting task, as \mathcal{S}_k is not necessarily at the beginning of the sequence.

3.3 Masked Autoregressive Modeling with Consistency Alignment

We aim to learn a generalized AR model that naturally unifies text and image conditions and adapts to panoramic characteristics. An intuitive solution is MAR modeling, which allows generation in arbitrary order by marking the position of each token. However, existing foundation models are typically pre-trained on perspective images and cannot cope with panoramic scenarios. We delve into this problem and use the cyclic translation equivariance of ERP panoramas.

Vanilla Architecture. We start with a vanilla text-conditioned MAR model [13] to learn basic image generation without special constraints. Specifically, we use continuous tokens instead of discrete ones to reduce quantization error.

As illustrated in Fig. 2 (a), panoramic images I are first compressed into latent representations x using a VAE encoder \mathcal{E} . These representations are fed into a transformer model f , which adopts an encoder-decoder architecture. Within the encoder, x is divided into a sequence of visual tokens via

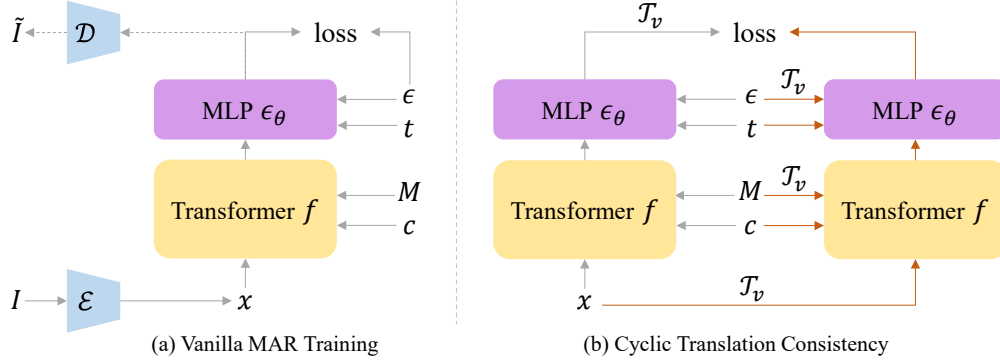


Figure 2: **Method illustration.** (a) PAR utilizes a transformer f to predict regions obscured by mask M , then employs these predictions as conditions to drive an MLP ϵ_θ in generating continuous tokens. The VAE encoder \mathcal{E} and decoder \mathcal{D} are frozen. The dashed line indicates the inference phase. c and t denote textual embeddings and time-steps, respectively. (b) Both original and \mathcal{T}_v -augmented triples (x, ϵ, M) are processed by the same model, and then aligned through a consistency loss.

patchification. A subset of these tokens is randomly masked by replacing the corresponding regions with a designated [MASK] token. Sine-cosine positional encodings (PEs) are added to the token sequence to preserve spatial information.

Simultaneously, textual prompts are processed by a pre-trained text encoder [25], which encodes them into textual embeddings $c \in \mathbb{R}^d$, where d matches the dimensionality of the visual tokens. The unmasked visual tokens are fused with the textual embeddings c in the encoder, and the resulting contextualized representations are then passed to the decoder, where they are integrated with the masked tokens to facilitate predictive reconstruction.

Unlike the standard AR modeling, the decoder’s output is not used as the final result, but as a conditional signal z to drive a lightweight denoising network, which is implemented by a three-layer multilayer perceptron (MLP) ϵ_θ . During the training phase, the noise-corrupted x_t is denoised by ϵ_θ under z as follows:

$$\mathcal{L}_{va} = \mathbb{E}_{t,\epsilon} [M \circ \|\epsilon_t - \epsilon_\theta(x_t|t, z)\|^2]. \quad (6)$$

In Eq. 6, \circ is pixel-wise multiplication with binary mask M , where the value corresponding to the masked token is 1. The encoder-decoder f and ϵ_θ are jointly optimized.

Cyclic Translation Consistency. Current foundation models [46, 13] are predominantly trained on perspective images, leading to suboptimal feature representations for ERP-formatted panoramas. We introduce a cyclic translation operator \mathcal{T}_v to address this domain gap and construct semantically equivalent panorama pairs, where v indicates arbitrary translation distance. As shown in Fig. 2 (b), we construct an input pair, (x, ϵ, M) and $(x', \epsilon', M') = (\mathcal{T}_v(x), \mathcal{T}_v(\epsilon), \mathcal{T}_v(M))$. Both inputs share identical PE maps to prevent trivial solutions. The main model processes these pairs to produce outputs y and y' , respectively. We enforce equivariance by aligning $\mathcal{T}_v(y)$ with y' only on masked regions through the objective:

$$\mathcal{L}_{consistency} = M' \circ \|\mathcal{T}_v(\epsilon_\theta(x_t|t, x, M)) - \epsilon_\theta(x'_t|t, x', M')\|^2, \quad (7)$$

The final learning objective can be written as follows:

$$\mathcal{L} = \mathcal{L}_{va} + \lambda \mathcal{L}_{consistency}, \quad (8)$$

where λ is set as 0.1 in our experiments.

Discussion. The equivariance constraint holds exclusively for ERP panoramas due to their inherent horizontal continuity. For perspective images, applying \mathcal{T}_v artificially creates discontinuous boundaries in the center of the shifted image, which violates two critical premises. 1) *Semantic equivalence.* Unlike panoramas, shifted perspective images lose semantic consistency due to non-periodic scene structures. 2) *Model prior.* Generation models inherently enforce feature continuity in image interiors, making it infeasible to produce fragmented content.

Circular Padding. While the AR model incorporates panoramic priors, the VAE’s latent space processing may still introduce discontinuities. Standard convolution operations in VAE provide

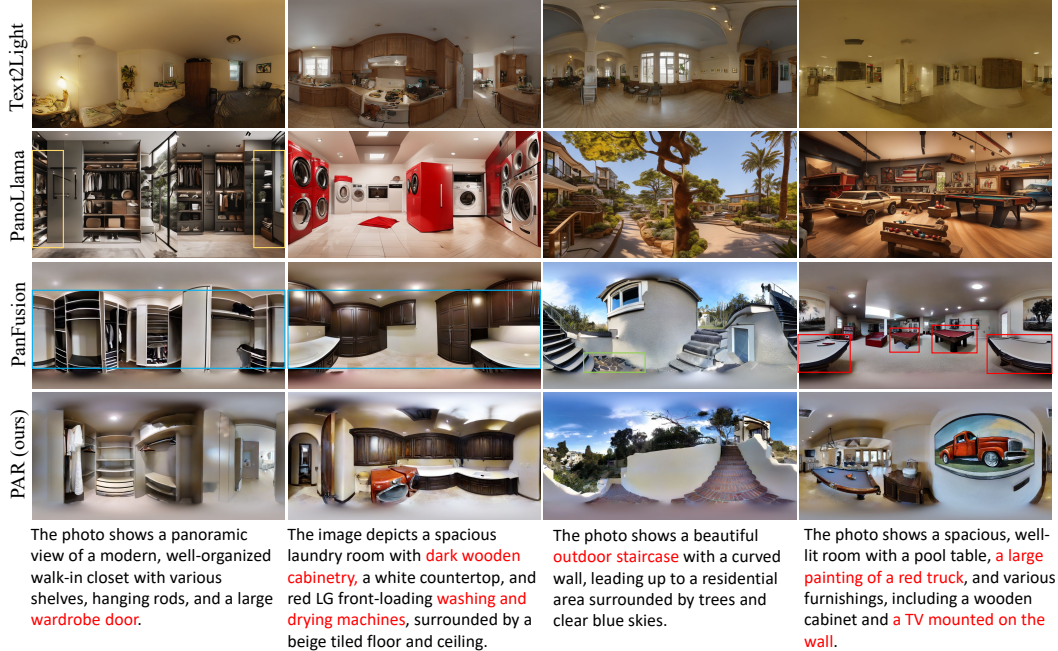


Figure 3: **Visual comparisons with previous methods on text-to-panorama task.** Previous methods neglect the circular consistency characteristics (yellow box), or suffer from repetitive objects (red box), artifact generation (blue box), and inconsistent combinations (green box). The highlighted portions in captions indicate text-image alignment failure cases of baseline methods.

Table 1: Performance on text-to-panorama task. PO and PE represent panorama outpainting and editing, respectively. **Bold** and underline indicate the first and second best entries.

Modeling	Method	#params	T2P	PO	PE	FAED ↓	FID ↓	CS ↑	DS ↓
Diffusion	PanFusion [71]	1.9B	✓	-	-	5.12	45.21	<u>31.07</u>	0.71
	Text2Light [9]	0.8B	✓	-	-	68.90	70.42	<u>27.90</u>	7.55
	PanoLlama [77]	0.8B	✓	-	-	33.15	103.51	32.54	13.99
AR	PAR (ours)	0.3B	✓	✓	✓	3.39	41.15	30.21	<u>0.58</u>
	PAR (ours)	0.6B	✓	✓	✓	3.34	<u>39.31</u>	30.34	0.57
	PAR (ours)	1.4B	✓	✓	✓	3.75	37.37	30.41	<u>0.58</u>

sufficient context for central regions but suffer from information asymmetry at image edges - pixels near boundaries receive unidirectional receptive fields. To address this issue, we propose a dual-space circular padding scheme: pre-padding and post-padding. The former is applied in pixel space for the VAE encoder, while the latter is used in latent space for the VAE decoder. Specifically, we crop a particular portion of the left and right regions and concatenate them to the other side, as formulated in Eq. 9.

$$C_r(x) = \text{concat}(x[\dots, -r * W/2], x, x[\dots, r * W/2]), \quad (9)$$

where $x \in \mathbb{R}^{H \times W}$ and $C_r(x) \in \mathbb{R}^{H \times (1+r)W}$, indicate the original and the padded tensor, respectively. r indicates the ratio of padding width to that of the original images or latent variables. After the VAE transformation, the edge positions have sufficient context information. Therefore, the areas that belong to the padding are discarded.

4 Experiment

4.1 Experiment Settings

Implementation Details. We utilize NOVA [13] as the initialization and set the resolution as 512×1024 . Our model is trained for 20K iterations with a batch size 32. We employ an AdamW



Figure 4: **Qualitative comparisons of panorama outpainting on the Matterport3D dataset.** PAR-1.4B is used for this task, where PAR w/o prompt means the textual prompt is set as empty.

Table 2: **Panorama outpainting results on the Matterport3D dataset.** For FID-h, we horizontally sample 8 perspective images with FoV=90° for each panorama and then calculate their FID.

Method	T2P	PO	PE	FID ↓	FID-h ↓
AOG-Net [35]	-	✓	-	83.02	37.88
2S-ODIS [37]	-	✓	-	52.59	35.18
PAR w/o prompt	✓	✓	✓	41.63	25.97
PAR w/ prompt	✓	✓	✓	32.68	12.20

optimizer [34]. The learning rate is 5×10^{-5} with the linear scheduler. In the inference stage, we set the CFG [22] coefficient as 5. In this paper, the masking sequence for training and the sampling sequence for inference are initialized with a uniform distribution unless otherwise stated.

Datasets and Metrics. We mainly use Matterport3D [5] for comparisons. The split of the training and validation set follows PanFusion [71]. We use Janus-Pro-7B [8] to generate the captions.

Several metrics are used in this paper. Fréchet Inception Distance (FID) [20] measures the similarity between the distribution of real and generated images in a feature space derived from a pre-trained inception network. Lower FID scores indicate better realism of images. CLIP Score (CS) [44] evaluates the alignment between text and image. Furthermore, as FID relies on an Inception network [52] trained on perspective images, we also report the Fréchet Auto-Encoder Distance (FAED) [39] score, which is a variant of FID customized for panorama. To measure the cycle consistency of panoramic images, we adopt Discontinuity Score (DS) [10].

Baselines. Since only a few approaches combine T2P and PO, we compare PAR with specialist methods separately. Specifically, for T2P, we compare with several diffusion-based and AR-based methods, including PanFusion [71], Text2Light [9], and PanoLlama [77]. We take AOG-Net [35] and 2S-ODIS [37] as PO baselines. All experiments are implemented on the Matterport3D dataset.

4.2 Main Results

Text-to-Panorama. Tab. 1 shows the quantitative comparison results. Within the scope of AR-based methods, our PAR significantly outperforms previous approaches regarding generation quality and continuity score. Our method is slightly inferior in the CS metric, probably because CLIP [44] is pre-trained on massive perspective images, and panoramic geometry is not well aligned with perspective images. Moreover, our model performs decently compared with a strong diffusion-based baseline, PanFusion, with only 0.3B parameters. Specifically, PAR-0.3B outperforms PanFusion with 1.73 and 4.06 on FAED and FID, with a discontinuity score of 0.58. Scaling up the parameters helps achieve better results, which is further illustrated in Sec. 4.3.

Fig. 3 provides visual comparisons with the aforementioned baseline methods, including diffusion-based and AR-based models. Our model shows better instruction-following ability, more consistent generation results, and avoids duplicate generation. Specifically, Text2Light cannot obtain satisfactory synthesized results. PanoLlama cannot understand panorama geometry and neglects the characteristic of cycle consistency. PanFusion produces more reasonable results, but sometimes faces artifact problems. For example, the first and second columns of the third row show a room without an exit.



Figure 5: **Scaling parameters and training compute improve fidelity and soundness.** Two cases are shown with 3 model sizes and 3 different training stages. From top to bottom: 0.3B, 0.6B, 1.4B. From left to right: 25%, 50%, 100% of the training process.



Figure 6: **Panorama outpainting on OOD dataset.** The images are from SUN360, which is out of the distribution of our training data. PAR generates realistic panorama images while previous methods have problems like artifacts, or unrealistic results.

Panorama Outpainting. Tab. 2 compares our method with AOG-Net and 2S-ODIS. We use the model trained with Eq. 8 and inference following Eq. 4, where \mathcal{S}_k indicates the positions within the mask. Our model achieves 32.68 and 12.20 on FID and FID-h, respectively. FID-h is similar to FID, but the difference is that it extracts eight perspective views in the horizontal direction with a 90-degree FoV for each panoramic image, which pays more attention to the generation quality of local regions. Fig. 4 visualizes the synthesized results. Existing methods suffer from local distortion (the 3rd column) or counterfactual repetitive structures (the 2nd column). Our method overcomes these problems and still produces reasonable results without textual prompts.

4.3 Ablation Study

Scalability. We train with three different parameter sizes, namely 0.3B, 0.6B, and 1.4B, respectively. In Tab. 1, FID and CS improve with increasing parameters. We also visualize the performance under different training stages, including 25%, 50%, and 100% of the whole training process. As shown in Fig. 5, the improvement of fidelity and soundness is consistent with the scaling of parameters and computation. Larger models learn data distributions better, such as details and panoramic geometry.

Generalization. Fig. 6 visualizes the outpainting results of PAR on OOD data. SUN360 [63] is used for evaluation, which has different data distributions from Matterport3D. PAR shows decent performance across various scenarios. We also compared with several PO baselines trained on the SUN360 dataset. However, Diffusion360 [17] suffers from realistic scenes and lacks details. Panodiff [59] also encounters artifact problems (red sky in the 1st row).

PAR can also adapt to different tasks, such as panoramic image editing. As shown in Fig. 7, the model needs to preserve the content inside the mask and regenerate according to new textual prompts. We designed three challenging text prompts, whose content differs from the training datasets, and contains specific conflicts with the original image. For example, fire vs. yard in (b), snow vs. current season of scene in (c), and ocean vs. current place of the scene in (d). Interestingly, our model can

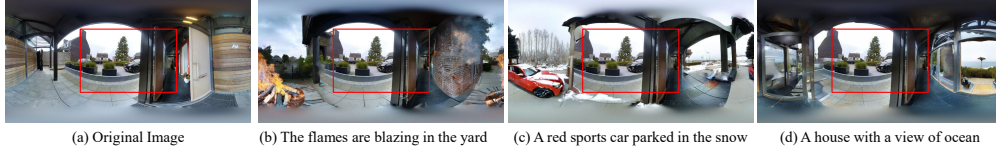


Figure 7: **Panoramic image editing.** We design several challenging textual prompts to enforce the model to regenerate the contents outside the red box while maintaining the inside contents. Note that our PAR performs zero-shot task generalization.

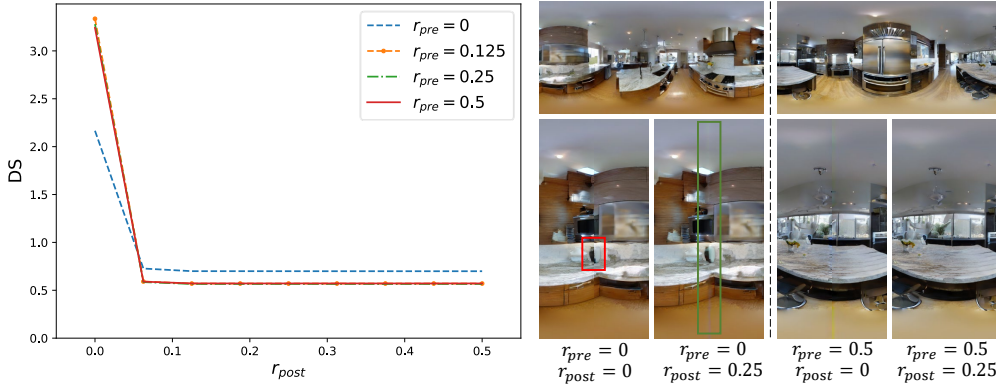


Figure 8: **Left:** The curve of DS about r_{post} . **Right:** Visualizations of different circular padding strategies. Each part consists of three images, where the top one represents the panoramic image generation result, the left and right ones represent the edge stitching results, respectively. The red box indicates the semantic discontinuity, and the green box highlights the seam after post-padding.

generate them well and understands panoramic characteristics. As shown in Fig. 7 (b), the left and right sides of the image can be stitched to form a whole fire.

Translation Equivariance. Tab. 3 demonstrates the effectiveness of consistency loss. Eq. 7 helps the model adapt to panoramic characteristics, thus improving generation quality. Fig. 8 (left) shows the convergence of r . Post-padding significantly improves DS when $r_{post} > 0$ as it helps to smooth stitching seams in the pixel space. However, the model without pre-padding suffers from higher discontinuity, indicating the misalignment between the training and testing phases. With the same r_{pre} , DS converges quickly when $r_{post} > 0.125$. A similar phenomenon is observed with r_{post} fixed. Specifically, the curve of $r_{pre} = 0.25$ and $r_{pre} = 0.5$ almost coincide.

Table 3: Ablations on cyclic consistency loss.

Method	FID ↓	CS ↑	DS ↓
w/o $\mathcal{L}_{consistency}$	39.55	30.25	0.57
w/ $\mathcal{L}_{consistency}$	37.37	30.41	0.58

Fig. 8 (right) visually explains the difference between the two padding strategies. When $r_{pre} = 0$, semantic inconsistency exists between the left and right edges of the panoramic image. Post-padding cannot repair it even with a large padding ratio, and the green box bounds the smoothed seam. In contrast, the model generates consistent contents when pre-padding is applied.

5 Conclusion

This paper proposes PAR, a MAR-based architecture unifying text and image-conditioned panoramic image generation. We delve into the cyclic translation equivariance of ERP panoramas and correspondingly propose a consistency alignment and circular padding strategy. Experiments demonstrate PAR’s effectiveness on text-to-panorama and panorama outpainting tasks, whilst showing promising scalability and generalization capability. We hope our research provides a new solution for the panorama generation community.

References

- [1] Omer Bar-Tal, Lior Yariv, Yaron Lipman, and Tali Dekel. Multidiffusion: Fusing diffusion paths for controlled image generation. In *ICML*, 2023. 2
- [2] Andreas Blattmann, Tim Dockhorn, Sumith Kulal, Daniel Mendelevitch, Maciej Kilian, Dominik Lorenz, Yam Levi, Zion English, Vikram Voleti, Adam Letts, et al. Stable video diffusion: Scaling latent video diffusion models to large datasets. *arXiv preprint arXiv:2311.15127*, 2023. 3
- [3] Tim Brooks, Aleksander Holynski, and Alexei A Efros. Instructpix2pix: Learning to follow image editing instructions. In *CVPR*, 2023. 3
- [4] Tom B. Brown, Benjamin Mann, Nick Ryder, Melanie Subbiah, Jared Kaplan, Prafulla Dhariwal, Arvind Neelakantan, Pranav Shyam, Girish Sastry, Amanda Askell, Sandhini Agarwal, Ariel Herbert-Voss, Gretchen Krueger, Tom Henighan, Rewon Child, Aditya Ramesh, Daniel M. Ziegler, Jeffrey Wu, Clemens Winter, Christopher Hesse, Mark Chen, Eric Sigler, Mateusz Litwin, Scott Gray, Benjamin Chess, Jack Clark, Christopher Berner, Sam McCandlish, Alec Radford, Ilya Sutskever, and Dario Amodei. Language models are few-shot learners. In *NeurIPS*, 2020. 3
- [5] Angel Chang, Angela Dai, Thomas Funkhouser, Maciej Halber, Matthias Niessner, Manolis Savva, Shuran Song, Andy Zeng, and Yinda Zhang. Matterport3d: Learning from rgb-d data in indoor environments. *arXiv preprint arXiv:1709.06158*, 2017. 2, 7
- [6] Huiwen Chang, Han Zhang, Jarred Barber, AJ Maschinot, Jose Lezama, Lu Jiang, Ming-Hsuan Yang, Kevin Murphy, William T Freeman, Michael Rubinstein, et al. Muse: Text-to-image generation via masked generative transformers. *arXiv preprint arXiv:2301.00704*, 2023. 3
- [7] Huiwen Chang, Han Zhang, Lu Jiang, Ce Liu, and William T Freeman. Maskgit: Masked generative image transformer. In *CVPR*, 2022. 3
- [8] Xiaokang Chen, Zhiyu Wu, Xingchao Liu, Zizheng Pan, Wen Liu, Zhenda Xie, Xingkai Yu, and Chong Ruan. Janus-pro: Unified multimodal understanding and generation with data and model scaling. *arXiv preprint arXiv:2501.17811*, 2025. 7
- [9] Zhaoxi Chen, Guangcong Wang, and Ziwei Liu. Text2light: Zero-shot text-driven hdr panorama generation. *ACM Transactions on Graphics*, 2022. 3, 6, 7
- [10] Anders Christensen, Nooshin Mojab, Khushman Patel, Karan Ahuja, Zeynep Akata, Ole Winther, Mar Gonzalez-Franco, and Andrea Colaco. Geometry fidelity for spherical images. In *ECCV*, 2024. 7
- [11] Thiago LT da Silveira, Paulo GL Pinto, Jeffri Murrugarra-Llerena, and Cláudio R Jung. 3d scene geometry estimation from 360 imagery: A survey. *ACM Computing Surveys*, 2022. 2
- [12] Mohammad Reza Karimi Dastjerdi, Yannick Hold-Geoffroy, Jonathan Eisenmann, Siavash Khodadadeh, and Jean-François Lalonde. Guided co-modulated gan for 360 field of view extrapolation. In *3DV*, 2022. 2
- [13] Haoge Deng, Ting Pan, Haiwen Diao, Zhengxiong Luo, Yufeng Cui, Huchuan Lu, Shiguang Shan, Yonggang Qi, and Xinlong Wang. Autoregressive video generation without vector quantization. *arXiv preprint arXiv:2412.14169*, 2024. 3, 4, 5, 6
- [14] Ming Ding, Zhuoyi Yang, Wenyi Hong, Wendi Zheng, Chang Zhou, Da Yin, Junyang Lin, Xu Zou, Zhou Shao, Hongxia Yang, et al. Cogview: Mastering text-to-image generation via transformers. In *NeurIPS*, 2021. 3
- [15] Ming Ding, Wendi Zheng, Wenyi Hong, and Jie Tang. Cogview2: Faster and better text-to-image generation via hierarchical transformers. In *NeurIPS*, 2022. 3
- [16] Patrick Esser, Sumith Kulal, Andreas Blattmann, Rahim Entezari, Jonas Müller, Harry Saini, Yam Levi, Dominik Lorenz, Axel Sauer, Frederic Boesel, et al. Scaling rectified flow transformers for high-resolution image synthesis. In *ICML*, 2024. 3
- [17] Mengyang Feng, Jinlin Liu, Miaomiao Cui, and Xuansong Xie. Diffusion360: Seamless 360 degree panoramic image generation based on diffusion models. *arXiv preprint arXiv:2311.13141*, 2023. 2, 8
- [18] Penglei Gao, Kai Yao, Tiandi Ye, Steven Wang, Yuan Yao, and Xiaofeng Wang. Opa-ma: Text guided mamba for 360-degree image out-painting. *arXiv preprint arXiv:2407.10923*, 2024. 2, 3
- [19] William Harvey, Saeid Naderiparizi, Vaden Masrani, Christian Weilbach, and Frank Wood. Flexible diffusion modeling of long videos. In *NeurIPS*, 2022. 3
- [20] Martin Heusel, Hubert Ramsauer, Thomas Unterthiner, Bernhard Nessler, and Sepp Hochreiter. Gans trained by a two time-scale update rule converge to a local nash equilibrium. In *NeurIPS*, 2017. 7
- [21] Jonathan Ho, Chitwan Saharia, William Chan, David J Fleet, Mohammad Norouzi, and Tim Salimans. Cascaded diffusion models for high fidelity image generation. *The Journal of Machine Learning Research*, 2022. 3
- [22] Jonathan Ho and Tim Salimans. Classifier-free diffusion guidance. In *NeurIPS Workshops*, 2021. 3, 7
- [23] Wenyi Hong, Ming Ding, Wendi Zheng, Xinghan Liu, and Jie Tang. Cogvideo: Large-scale pretraining for text-to-video generation via transformers. *arXiv preprint arXiv:2205.15868*, 2022. 3
- [24] Kuan-Chih Huang, Xiangtai Li, Lu Qi, Shuicheng Yan, and Ming-Hsuan Yang. Reason3d: Searching and reasoning 3d segmentation via large language model. In *3DV*, 2025. 2

- [25] Mojan Javaheripi, Sébastien Bubeck, Marah Abdin, Jyoti Aneja, Sebastien Bubeck, Caio César Teodoro Mendes, Weizhu Chen, Allie Del Giorno, Ronen Eldan, Sivakanth Gopi, et al. Phi-2: The surprising power of small language models. *Microsoft Research Blog*, 2023. 5
- [26] Nikolai Kalischek, Michael Oechsle, Fabian Manhardt, Philipp Henzler, Konrad Schindler, and Federico Tombari. Cubediff: Repurposing diffusion-based image models for panorama generation. *arXiv preprint arXiv:2501.17162*, 2025. 2, 3
- [27] Dan Kondratyuk, Lijun Yu, Xiuye Gu, José Lezama, Jonathan Huang, Rachel Hornung, Hartwig Adam, Hassan Akbari, Yair Alon, Vighnesh Birodkar, et al. Videopoet: A large language model for zero-shot video generation. *arXiv preprint arXiv:2312.14125*, 2023. 3
- [28] Jialu Li and Mohit Bansal. Panogen: Text-conditioned panoramic environment generation for vision-and-language navigation. In *NeurIPS*, 2023. 2, 3
- [29] Tianhong Li, Yonglong Tian, He Li, Mingyang Deng, and Kaiming He. Autoregressive image generation without vector quantization. In *NeurIPS*, 2024. 2, 3
- [30] Yaron Lipman, Ricky TQ Chen, Heli Ben-Hamu, Maximilian Nickel, and Matt Le. Flow matching for generative modeling. In *ICLR*, 2023. 3
- [31] Xingchao Liu, Chengyue Gong, and Qiang Liu. Flow straight and fast: Learning to generate and transfer data with rectified flow. In *ICLR*, 2023. 3
- [32] Xingchao Liu, Xiwen Zhang, Jianzhu Ma, Jian Peng, et al. InstafLOW: One step is enough for high-quality diffusion-based text-to-image generation. In *ICLR*, 2024. 3
- [33] Yuheng Liu, Xinke Li, Xueting Li, Lu Qi, Chongshou Li, and Ming-Hsuan Yang. Pyramid diffusion for fine 3d large scene generation. In *ECCV*, 2024. 2
- [34] Ilya Loshchilov, Frank Hutter, et al. Fixing weight decay regularization in adam. *arXiv preprint arXiv:1711.05101*, 2017. 7
- [35] Zhuqiang Lu, Kun Hu, Chaoyue Wang, Lei Bai, and Zhiyong Wang. Autoregressive omni-aware outpainting for open-vocabulary 360-degree image generation. In *AAAI*, 2024. 2, 3, 7
- [36] Andreas Lugmayr, Martin Danelljan, Andres Romero, Fisher Yu, Radu Timofte, and Luc Van Gool. Repaint: Inpainting using denoising diffusion probabilistic models. In *CVPR*, 2022. 3
- [37] Atsuya Nakata and Takao Yamanaka. 2s-odis: Two-stage omni-directional image synthesis by geometric distortion correction. In *ECCV*, 2024. 7
- [38] Charlie Nash, Joao Carreira, Jacob Walker, Iain Barr, Andrew Jaegle, Mateusz Malinowski, and Peter Battaglia. Transframer: Arbitrary frame prediction with generative models. *arXiv preprint arXiv:2203.09494*, 2022. 3
- [39] Changyoon Oh, Wonjune Cho, Yujeong Chae, Daehee Park, Lin Wang, and Kuk-Jin Yoon. Bips: Bi-modal indoor panorama synthesis via residual depth-aided adversarial learning. In *ECCV*, 2022. 7
- [40] William Peebles and Saining Xie. Scalable diffusion models with transformers. In *ICCV*, 2023. 3
- [41] Dustin Podell, Zion English, Kyle Lacey, Andreas Blattmann, Tim Dockhorn, Jonas Müller, Joe Penna, and Robin Rombach. Sdxl: Improving latent diffusion models for high-resolution image synthesis. In *ICLR*, 2024. 2, 3
- [42] Lu Qi, Li Jiang, Shu Liu, Xiaoyong Shen, and Jiaya Jia. Amodal instance segmentation with kins dataset. In *CVPR*, 2019. 2
- [43] Yu Qiu, Xin Lin, Jingbo Wang, Xiangtai Li, Lu Qi, and Ming-Hsuan Yang. Umc: Unified resilient controller for legged robots with joint malfunctions. In *arXiv*, 2025. 2
- [44] Alec Radford, Jong Wook Kim, Chris Hallacy, Aditya Ramesh, Gabriel Goh, Sandhini Agarwal, Girish Sastry, Amanda Askell, Pamela Mishkin, Jack Clark, et al. Learning transferable visual models from natural language supervision. In *ICML*, 2021. 7
- [45] Aditya Ramesh, Mikhail Pavlov, Gabriel Goh, Scott Gray, Chelsea Voss, Alec Radford, Mark Chen, and Ilya Sutskever. Zero-shot text-to-image generation. In *ICML*, 2021. 3
- [46] Robin Rombach, Andreas Blattmann, Dominik Lorenz, Patrick Esser, and Björn Ommer. High-resolution image synthesis with latent diffusion models. In *CVPR*, 2022. 2, 3, 5
- [47] Chitwan Saharia, William Chan, Huiwen Chang, Chris Lee, Jonathan Ho, Tim Salimans, David Fleet, and Mohammad Norouzi. Palette: Image-to-image diffusion models. In *SIGGRAPH*, 2022. 3
- [48] Chitwan Saharia, Jonathan Ho, William Chan, Tim Salimans, David J Fleet, and Mohammad Norouzi. Image super-resolution via iterative refinement. *TPAMI*, 2022. 3
- [49] Jiaming Song, Chenlin Meng, and Stefano Ermon. Denoising diffusion implicit models. In *ICLR*, 2021. 3
- [50] Yang Song, Jascha Sohl-Dickstein, Diederik P Kingma, Abhishek Kumar, Stefano Ermon, and Ben Poole. Score-based generative modeling through stochastic differential equations. In *ICLR*, 2021. 3
- [51] Peize Sun, Yi Jiang, Shoufa Chen, Shilong Zhang, Bingyue Peng, Ping Luo, and Zehuan Yuan. Autoregressive model beats diffusion: Llama for scalable image generation. *arXiv preprint arXiv:2406.06525*, 2024. 3
- [52] Christian Szegedy, Vincent Vanhoucke, Sergey Ioffe, Jon Shlens, and Zbigniew Wojna. Rethinking the inception architecture for computer vision. In *CVPR*, 2016. 7

- [53] Jing Tan, Shuai Yang, Tong Wu, Jingwen He, Yuwei Guo, Ziwei Liu, and Dahua Lin. Imagine360: Immersive 360 video generation from perspective anchor. *arXiv preprint arXiv:2412.03552*, 2024. 2, 3
- [54] Shitao Tang, Jiacheng Chen, Dilin Wang, Chengzhou Tang, Fuyang Zhang, Yuchen Fan, Vikas Chandra, Yasutaka Furukawa, and Rakesh Ranjan. Mvdifffusion++: A dense high-resolution multi-view diffusion model for single or sparse-view 3d object reconstruction. In *ECCV*, 2024. 2
- [55] Shitao Tang, Fuyang Zhang, Jiacheng Chen, Peng Wang, and Yasutaka Furukawa. Mvdifffusion: Enabling holistic multi-view image generation with correspondence-aware diffusion. In *NeurIPS*, 2023. 2, 3
- [56] Hugo Touvron, Louis Martin, Kevin Stone, Peter Albert, Amjad Almahairi, Yasmine Babaei, Nikolay Bashlykov, Soumya Batra, Prajjwal Bhargava, Shruti Bhosale, et al. Llama 2: Open foundation and fine-tuned chat models. *arXiv: 2307.09288*, 2023. 3
- [57] Ruben Villegas, Mohammad Babaeizadeh, Pieter-Jan Kindermans, Hernan Moraldo, Han Zhang, Mohammad Taghi Saffar, Santiago Castro, Julius Kunze, and Dumitru Erhan. Phenaki: Variable length video generation from open domain textual descriptions. In *ICLR*, 2022. 3
- [58] Zhaoliang Wan, Yonggen Ling, Senlin Yi, Lu Qi, Wangwei Lee, Minglei Lu, Sicheng Yang, Xiao Teng, Peng Lu, Xu Yang, et al. Vint-6d: A large-scale object-in-hand dataset from vision, touch and proprioception. In *ICML*, 2024. 2
- [59] Jionghao Wang, Ziyu Chen, Jun Ling, Rong Xie, and Li Song. 360-degree panorama generation from few unregistered nfov images. *arXiv preprint arXiv:2308.14686*, 2023. 2, 8
- [60] Yuqing Wang, Tianwei Xiong, Daquan Zhou, Zhijie Lin, Yang Zhao, Bingyi Kang, Jiashi Feng, and Xihui Liu. Loong: Generating minute-level long videos with autoregressive language models. *arXiv preprint arXiv:2410.02757*, 2024. 3
- [61] Tao Wu, Xuewei Li, Zhongang Qi, Di Hu, Xintao Wang, Ying Shan, and Xi Li. Spherediffusion: Spherical geometry-aware distortion resilient diffusion model. In *AAAI*, 2024. 2
- [62] Tianhao Wu, Chuanxia Zheng, and Tat-Jen Cham. Panodiffusion: 360-degree panorama outpainting via diffusion. *arXiv preprint arXiv:2307.03177*, 2023. 2
- [63] Jianxiong Xiao, Krista A Ehinger, Aude Oliva, and Antonio Torralba. Recognizing scene viewpoint using panoramic place representation. In *CVPR*, 2012. 8
- [64] Wilson Yan, Yunzhi Zhang, Pieter Abbeel, and Aravind Srinivas. Videogpt: Video generation using vq-vae and transformers. *arXiv preprint arXiv:2104.10157*, 2021. 3
- [65] Liu Yang, Huiyu Duan, Yucheng Zhu, Xiaohong Liu, Lu Liu, Zitong Xu, Guangji Ma, Xiongkuo Min, Guangtao Zhai, and Patrick Le Callet. Omni²: Unifying omnidirectional image generation and editing in an omni model. *arXiv preprint arXiv:2504.11379*, 2025. 2, 3
- [66] Ruihan Yang, Prakhar Srivastava, and Stephan Mandt. Diffusion probabilistic modeling for video generation. *Entropy*, 2023. 3
- [67] Weicai Ye, Chenhao Ji, Zheng Chen, Junyao Gao, Xiaoshui Huang, Song-Hai Zhang, Wanli Ouyang, Tong He, Cairong Zhao, and Guofeng Zhang. Diffpano: Scalable and consistent text to panorama generation with spherical epipolar-aware diffusion. *arXiv preprint arXiv:2410.24203*, 2024. 2
- [68] Fanghua Yu, Jinjin Gu, Zheyuan Li, Jinfan Hu, Xiangtao Kong, Xintao Wang, Jingwen He, Yu Qiao, and Chao Dong. Scaling up to excellence: Practicing model scaling for photo-realistic image restoration in the wild. In *CVPR*, 2024. 3
- [69] Jiahui Yu, Yuanzhong Xu, Jing Yu Koh, Thang Luong, Gunjan Baid, Zirui Wang, Vijay Vasudevan, Alexander Ku, Yinfei Yang, Burcu Karagol Ayan, et al. Scaling autoregressive models for content-rich text-to-image generation. *arXiv preprint arXiv:2206.10789*, 2022. 3
- [70] Lijun Yu, Yong Cheng, Kihyuk Sohn, José Lezama, Han Zhang, Huiwen Chang, Alexander G Hauptmann, Ming-Hsuan Yang, Yuan Hao, Irfan Essa, et al. Magvit: Masked generative video transformer. In *CVPR*, 2023. 3
- [71] Cheng Zhang, Qianyi Wu, Camilo Cruz Gambardella, Xiaoshui Huang, Dinh Phung, Wanli Ouyang, and Jianfei Cai. Taming stable diffusion for text to 360 panorama image generation. In *CVPR*, 2024. 2, 3, 6, 7
- [72] Lvmin Zhang, Anyi Rao, and Maneesh Agrawala. Adding conditional control to text-to-image diffusion models. In *ICCV*, 2023. 3
- [73] Lvmin Zhang, Anyi Rao, and Maneesh Agrawala. Scaling in-the-wild training for diffusion-based illumination harmonization and editing by imposing consistent light transport. In *ICLR*, 2025. 3
- [74] Xiaoyu Zhang, Teng Zhou, Xinlong Zhang, Jia Wei, and Yongchuan Tang. Multi-scale diffusion: Enhancing spatial layout in high-resolution panoramic image generation. *arXiv preprint arXiv:2410.18830*, 2024. 2
- [75] Dian Zheng, Cheng Zhang, Xiao-Ming Wu, Cao Li, Chengfei Lv, Jian-Fang Hu, and Wei-Shi Zheng. Panorama generation from nfov image done right. *arXiv preprint arXiv:2503.18420*, 2025. 2
- [76] Junwei Zhou, Xueting Li, Lu Qi, and Ming-Hsuan Yang. Layout-your-3d: Controllable and precise 3d generation with 2d blueprint. In *ICLR*, 2025. 2
- [77] Teng Zhou, Xiaoyu Zhang, and Yongchuan Tang. Panollama: Generating endless and coherent panoramas with next-token-prediction llms. *arXiv preprint arXiv:2411.15867*, 2024. 3, 6, 7